COMMUNICATION

Record figure of merit values of highly stoichiometric Sb$_2$Te$_3$ porous bulk synthesized from tailor-made molecular precursors in ionic liquids

Stefan Heimann,[a] Stephan Schulz,*[b] Julian Schaumann,[c] Anja Mudring,*[cd] Julia Stötzel,[e] Franziska Maculewicz[e] and Gabi Schierning*[f]

We report on the synthesis of Sb$_2$Te$_3$ nanoparticles with record-high figure of merit values of up to 1.5. The central thermoelectric parameters, electrical conductivity, thermal conductivity and Seebeck coefficient, were independently optimized. The critical influence of porosity for the fabrication of highly efficient thermoelectric materials is firstly demonstrated, giving a strong guidance for the optimization of other thermoelectric materials.

Thermoelectric materials directly convert heat fluxes into useable electricity and are therefore discussed as a key-enabler in waste heat recovery. For this vision, the main challenge is to develop thermoelectric materials with sufficiently high conversion efficiencies, expressed by the material's figure of merit $zT = \alpha^2\sigma T/\kappa$, where α, σ, κ and T are Seebeck coefficient, electrical conductivity, thermal conductivity, and temperature, respectively. $\alpha^2\sigma$ is called power factor. It is assumed that $zT \cong 1.5$ is necessary for most technical applications.[1]

Nanostructuring of thermoelectric materials has been demonstrated experimentally and theoretically to greatly improve the figure of merit by reducing the lattice contribution to the thermal conductivity.[2,3] Different types of scattering centers for the heat carrying phonons were implemented as design concepts for thermoelectric materials, such as nanoscale precipitates or interfaces.[4,5] To effectively scatter the broad spectrum of phonon wavelengths,

a hierarchical design of the nano- and microstructure was developed which led to record-high zT values.[6]

On the other hand, an increase of disorder in the nano- and microstructure of a crystal simultaneously increases the charge carrier scattering, which limits the nano- and microstructuring approach since the charge carrier mobility gets affected adversely. A high electrical conductivity further requires a high charge carrier concentration. The latter compromises the Seebeck coefficient which is best when the charge carrier concentration is low. Thus, to optimize a thermoelectric material, a careful decoupling of the competing and interrelated thermoelectric transport coefficients is mandatory.

We herein report on a strategy that allows to individually address and optimize each of the three thermoelectric transport coefficients in the nanobulk fabrication process as demonstrated for a standard thermoelectric material, Sb$_2$Te$_3$. Synergistic effects result in a dramatic enhancement of zT up to 1.5 around 300 °C. This specific versatile approach opens up a new synthetic strategy to a general route to highly efficient thermoelectric materials.

Control of the charge carrier concentration is the first important aspect in optimizing the performance of a thermoelectric material. Metal chalcogenides such as Sb$_2$Te$_3$ have a phase width (are not line compounds) and are intrinsically doped by anti-site defects. As a consequence, the Seebeck coefficient of Sb$_2$Te$_3$ obtained by traditional synthetic approaches tends to be lower than required for thermoelectric application. Thus, the anti-site defect concentration needs to be carefully adjusted since too many defects result in a sub-optimal charge carrier concentration. To control the composition and the anti-site defect concentration we employ a molecular single-source precursor, which provides Sb and Te in the correct stoichiometric ratios. By its thermal decomposition we yield highly stoichiometric Sb$_2$Te$_3$ nanoparticles with a defined defect concentration and high Seebeck coefficients.

The second aspect to take into account when optimizing a thermoelectric material is the carrier mobility: the electrical mobility of nanocomposites is often compromised not only by the nanostructure itself but by the incorporation of impurities, arising from the use of surfactants which were chosen to stabilize

[a] *Faculty of Chemistry, University of Duisburg-Essen, DE-45117, Essen, Germany*

[b] *Faculty of Chemistry and Center for NanoIntegration (CENIDE), University of Duisburg-Essen, DE-45117, Essen, Germany. E-mail: stephan.schulz@uni-due.de*

[c] *Inorganic Chemistry III – Materials Engineering and Characterization, Ruhr-Universität Bochum, DE-44780, Bochum, Germany*

[d] *Materials Science and Engineering, Iowa State University and Critical Materials Institute, Ames Laboratory, Ames, IA, 50011, USA. E-mail: mudring@iastate.edu*

[e] *Faculty of Engineering, University of Duisburg-Essen, Bismarckstr. 81, DE-47057, Duisburg, Germany*

[f] *Faculty of Engineering and Center for NanoIntegration (CENIDE), University of Duisburg-Essen, Bismarckstr. 81, DE-47057, Duisburg, Germany. E-mail: gabi.schierning@uni-due.de*

† Electronic supplementary information (ESI) available. See DOI: 10.1039/c5tc01248a

This journal is © The Royal Society of Chemistry 2015

J. Mater. Chem. C, 2015, **3**, 10375–10380 | **10375**

the nanostructure, but are now limiting the carrier mobility, especially at the grain boundaries. For that reason, we chose a synthesis approach which promises as far as possible an impurity free product: the decomposition of the single-source precursor in an ionic liquid under the influence of microwaves. The ionic liquid serves a threefold purpose: it acts as the solvent and nanoparticle stabilizer as well as the heat-transfer medium. Coupling ionic liquids with microwave heating leads to an extremely efficient energy uptake resulting in short reaction times which favors particle formation rather than particle growth.[7] At the same time the nanoparticles are sterically and electrostatically shielded by the ionic liquid against agglomeration and further particle growth.[8] Nevertheless, as our previous investigations show the ionic liquid can easily be removed by a simple washing procedure, as they are, compared to standard nanoparticle stabilizers weakly coordinating.[9] Thus, this guarantees a relatively clean, impurity free particle surface which puts no additional burden on the carrier mobility and leads to an optimization of the electric conductivity.

Finally, in order to tune the thermal conductivity of the material, we chose porosity as a design principle. It is known that phonon-boundary scattering at pores effectively reduces the mean free path of phonons. A high porosity of the compacted nanostructured material could be obtained by applying a mild compaction process consisting of cold pressing and subsequent annealing.[10,11]

As we will discuss in detail in the following, conceptually addressing all three thermoelectric transport coefficients individually in the manufacturing process of a thermoelectric material leads to dramatic enhancement of the figure of merit (Fig. 1).

Sb_2Te_3 typically exhibits a strong tendency to form anti-site defects and off-stoichiometric compositions lead to a reduced Seebeck coefficient.[12,13] Using single-source precursors allows to access to highly stoichiometric materials as we and others recently demonstrated.[14,15] We identified $(Et_2Sb)_2Te$ as the most promising precursor due to its clean, stoichiometric decomposition to Sb_2Te_3 and volatile $SbEt_3$ under mild conditions (140–180 °C). The wet chemical synthesis of Sb_2Te_3 nanoparticles by thermal decomposition of $(Et_2Sb)_2Te$ in standard organic solvents already proved our concept to optimize the Seebeck coefficient, which was found to range from 145 $\mu V\ K^{-1}$ to 170 $\mu V\ K^{-1}$.[14] These values are close to optimized values of bulk materials,[16] demonstrating a low defect density and low carrier densities in the order of 10^{19} to $10^{20}\ cm^{-3}$. Moreover, the thermal conductivity of only 0.29 to 0.27 W $m^{-1}\ K^{-1}$ was much lower compared to that of single crystalline Sb_2Te_3.[17] However, the use of specific capping agents (PVP*) compromised the electrical conductivity dramatically. While the molecular precursor determines the charge carrier concentration of the material due to the formation of highly stoichiometric material, the mobility of the charge carriers suffers from impurities which are incorporated into the material due to the capping agents.

Therefore, in order to optimize the electrical conductivity of the Sb_2Te_3 material, a different strategy to synthesize nanomaterials from the single source precursor was necessary. As outlined before, ionic liquids offer several advantages in the synthesis of nanoparticles by microwave irradiation. They allow for efficient size- and shape control due to their property to stabilize the surface of the growing nanoparticle,[18] yet, in contrast to standard capping agents, ILs can be easily removed from the nanoparticle surface.[19] The high microwave susceptibility of
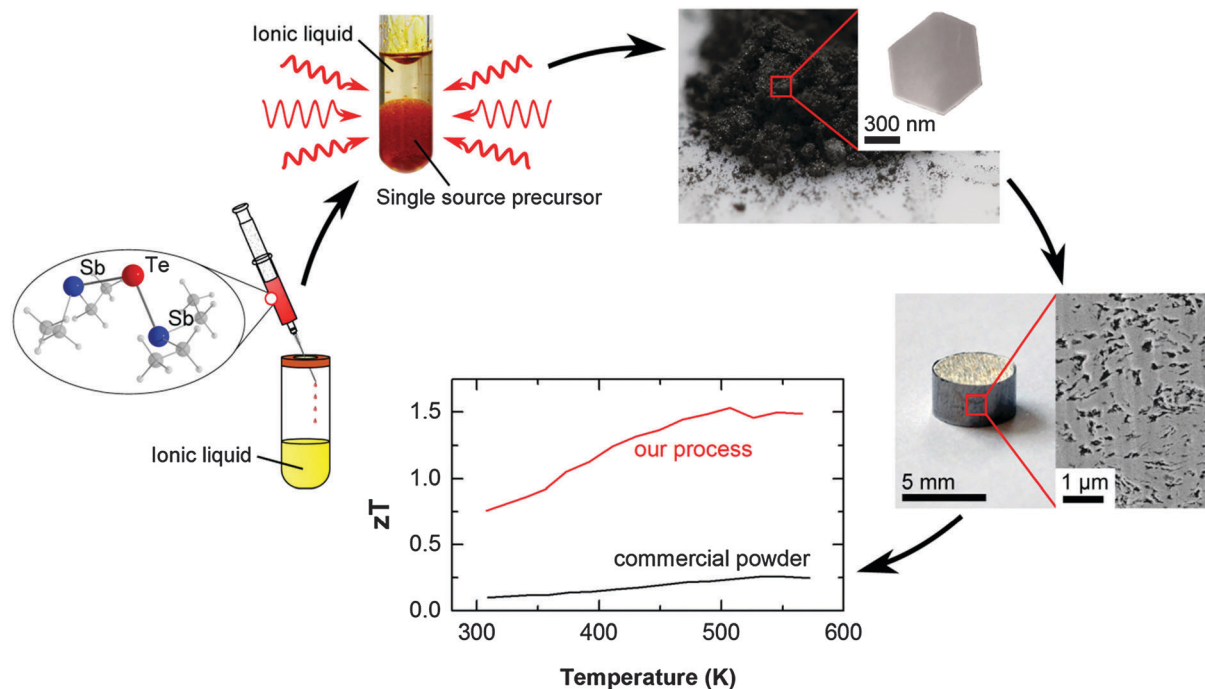

Fig. 1 Sketch of the manufacturing process: a single-source precursor is decomposed in an ionic liquid by microwave heating. Pellets are processed by a mild compaction and subsequent annealing.

ionic liquids enables a fast reaction within only a few minutes instead of several hours when compared to conventional methods such as classical thermal decomposition in a solvent which leaves more time for particle growth.[20]

Different ionic liquids with various cations and anions were systematically screened (see ESI†). They were selected to screen over a wide range of sizes and ion potential, Lewis acidity and basicity as well as coordination modes. In addition, the respective cation–anion combination of the ionic liquid also determines the melting point and viscosity which are important parameters in the synthesis. To prove the benefit of the microwave-assisted decomposition of the single-source precursor we carried out classical thermal decomposition experiments. In summary, $[C_4mim]Br$ (C_4mim = 1-butyl-3-methylimidzolium) as the ionic liquid combined with microwave heating proved to give the best results. Hereby, in order to obtain high performance thermoelectric material, the most important criteria for the choice of the IL were the requirement that the Sb_2Te_3 nanoparticle-agglomerates have to be phase-pure and provide a very clean particle surface. IR and EDX proved that the particle surface was free from any organic contaminations such as oxygen and carbon.

While the electronic transport properties are tuned by the choice of the molecular precursor as well as the nanoparticle fabrication process, the thermal conductivity reflects the structural peculiarities of the compacted bulk. Phonon-boundary scattering effectively reduces the thermal conductivity. Hereby, scattering at interfaces between adjacent nanoparticles and agglomerates as well as scattering at pores both contributes to a reduction of the phononic part of the thermal conductivity. Interfaces as well as pores both can create scattering events for electrons, too.

Hence, such structural inhomogeneities can only be used to tailor the thermal transport of materials which contain very good transport paths for electrons. Given such favorable electronic properties as precondition, porosity can be used for a figure of merit optimization as was demonstrated for porous silicon meshes with extraordinarily high zT values:[21,22] single crystalline silicon membranes with nanoscopic holes feature a drastically reduced mean free path of the phonons, reducing the thermal conductivity efficiently. As shown for these porous membranes, this design strategy has only a minor impact on the electrical conductivity, and very high values of the figure of merit were achieved.

Consequently, nanostructured bulk samples with varying density were produced applying a mild compaction process (cold pressing followed by annealing) to the Sb_2Te_3 nanopowder. The geometric density of the resulting materials was found to range between 76% up to 87% of the theoretical density. Fig. 2 shows characteristic scanning electron microscopy (SEM) images of an isolated nanoparticle, nanoparticle-agglomerates, and cross sections of the porous bulk samples.

Thermoelectric transport properties of two different samples, one where the single-source precursor was decomposed in an IL under microwaves (sample I), and material yielded through thermal decomposition in an oil bath (sample II) are compared in Fig. 3. Both samples have excellent Seebeck coefficients (Fig. 3A, 180 $\mu V K^{-1}$ at RT) proving the formation of a highly stoichiometric Sb_2Te_3 with low anti-site defect concentrations as intended by the use of the single-source precursor. The charge carrier concentration obtained from Hall measurements was between 4×10^{19} cm^{-3} and 5×10^{19} cm^{-3} for both samples and
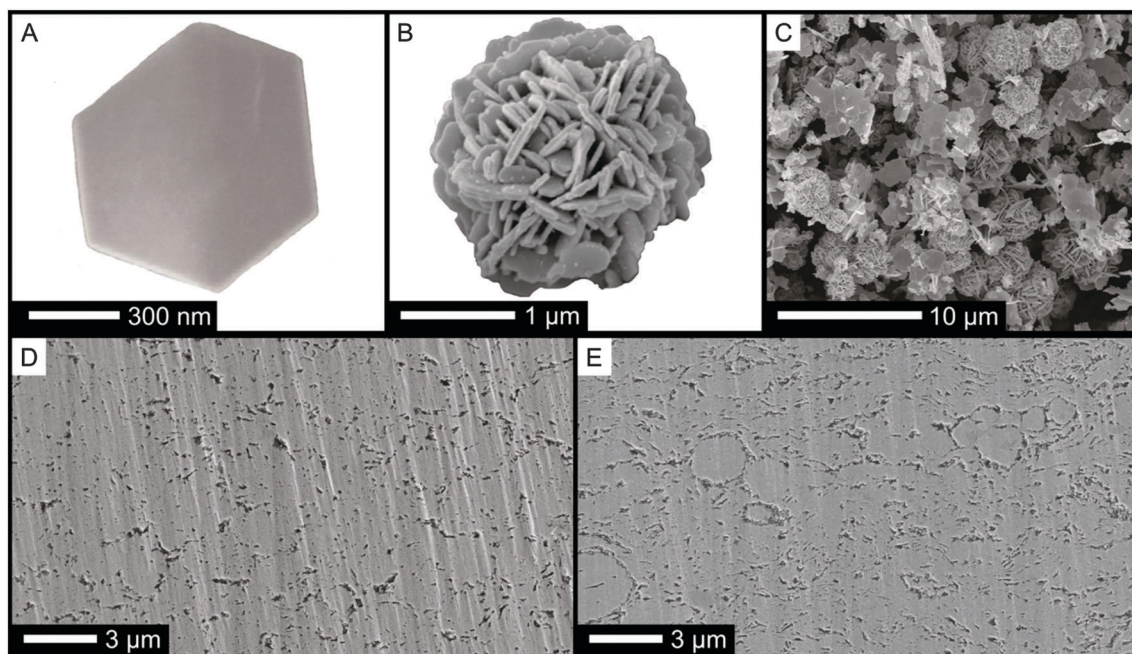

Fig. 2 SEM images of a single Sb_2Te_3 nanoparticle (A), an isolated agglomerate (B) and the powder containing many of such agglomerates (C). Cross sections of two cold pressed pellets decomposed in the microwave for 5 min (sample I) with many agglomerates preserved within the microstructure (D) and in an oil bath for 4 h (sample II) showing only a few agglomerates in the microstructure (E).
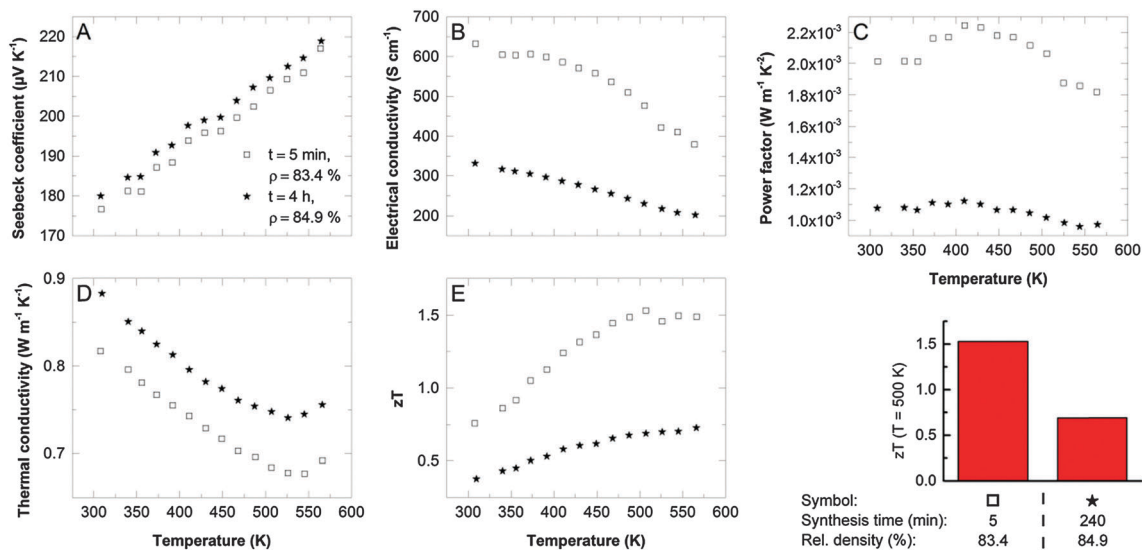
This journal is © The Royal Society of Chemistry 2015

J. Mater. Chem. C, 2015, 3, 10375–10380 | 10377

Fig. 3 Thermoelectric transport properties of two different Sb_2Te_3 nanoporous bulk samples, synthesized at 170 °C either within 5 minutes in IL using a microwave reactor (sample I, □) or within 4 hours by thermal decomposition in an oil bath (sample II, *).

therewith close to ideal for Sb_2Te_3.[17] The electrical conductivity (Fig. 3B) correlates with the reaction time: with increasing reaction time, the incorporation of impurities such as oxygen or carbon (decomposition of as-formed $SbEt_3$) becomes more likely resulting in a reduced electrical conductivity. This is reflected by the charge carrier mobility which is 42 cm^2 V^{-1} s^{-1} for sample II (thermal decomposition in an oil bath) and 130 cm^2 V^{-1} s^{-1} for sample I (microwave reactor combined with IL). High power factors of $>2 \times 10^{-3}$ W m^{-1} K^{-2} are the consequence for an optimized sample (Fig. 3C). Unexpectedly, the thermal conductivity of the two samples shows an opposite trend compared to the electrical conductivity. The shorter reaction time results not only in the higher electrical conductivity but also in the lower thermal conductivity. The origin may be found in the different size and shape of the nanoparticle-agglomerates produced by the different processes: a high number of spherical agglomerates larger than 2 μm were obtained in the microwave process. Polished cross sections of the compacted bulk samples give indications that these agglomerates are preserved in the pellets after annealing (Fig. 2D and E). We speculate that a good electronic transport is possible within the agglomerates due to the intimate contact of the nanoplates whereas the high number of interfaces may reduce the phonon transport. Moreover, the density of the pellets slightly differs: the increasing number of agglomerates results in an increasing porosity.

To evaluate the role of porosity in more detail, we fabricated a series of samples from commercial Sb_2Te_3 powder (Alfa Aesar) by cold pressing, applying different pressure and subsequent annealing in an identical way as before. Consequently, these samples vary in the relative density between 79% and 90% and their thermoelectric transport properties are shown in Fig. 4.

The Seebeck coefficient (Fig. 4A) is mostly dominated by the anti-site defect concentration of the Sb_2Te_3 starting material and is therefore almost identical for the three samples. In comparison, using the single-source precursor increased the

Seebeck coefficient by 40% due to the control of the anti-site defects concentration.

The electrical conductivity most likely suffers from impurities as was observed for our sample II (4 h conventional heating), hence resulting in power factors almost one order of magnitude smaller than for our optimized process. The most prominent impact of the compaction process addresses the thermal conductivity which perfectly correlates with the porosity of the samples: the higher the porosity, the lower the thermal conductivity. Usually, the electrical conductivity is also reduced by introducing pores into the microstructure, but this effect is less pronounced, especially at densities below 85% (Fig. 4B). The overall figure of merit obtained for the commercial powder did not exceed 0.3 at 300 °C.

Our results demonstrate the efficiency of our new concept which is based on the decoupling of electronic and phononic transport properties, resulting in a dramatic enhancement of the figure of merit of best 1.5 at 300 °C. Thermal decomposition of a suitable single-source precursor in the presence of organic capping agents resulted in high Seebeck coefficients but a disappointing figure of merit (below 0.1 due to low electrical conductivity).[14] In remarkable contrast, fast microwave-assisted decomposition of the single-source precursor in an ionic liquid substantially improved the electrical conductivity, hence improving the powder factors and the figure of merit of up to 1. Finally, controlling the porosity of the nanostructured material yielded record high zT values of up to 1.5 (compare Fig. 5), without the need of alloying or electronic doping.

We have demonstrated the key role of porosity for the enhancement of the thermoelectric figure of merit which can be applied as tuning parameter for materials with excellent electronic properties. This rather simple synthesis approach can likely be transferred to other type of thermoelectric materials such as other metal chalcogenides and their alloys. Moreover, electronic co-doping of Sb_2Te_3 with e.g. sulphur or titanium can

10378 | J. Mater. Chem. C, 2015, **3**, 10375–10380

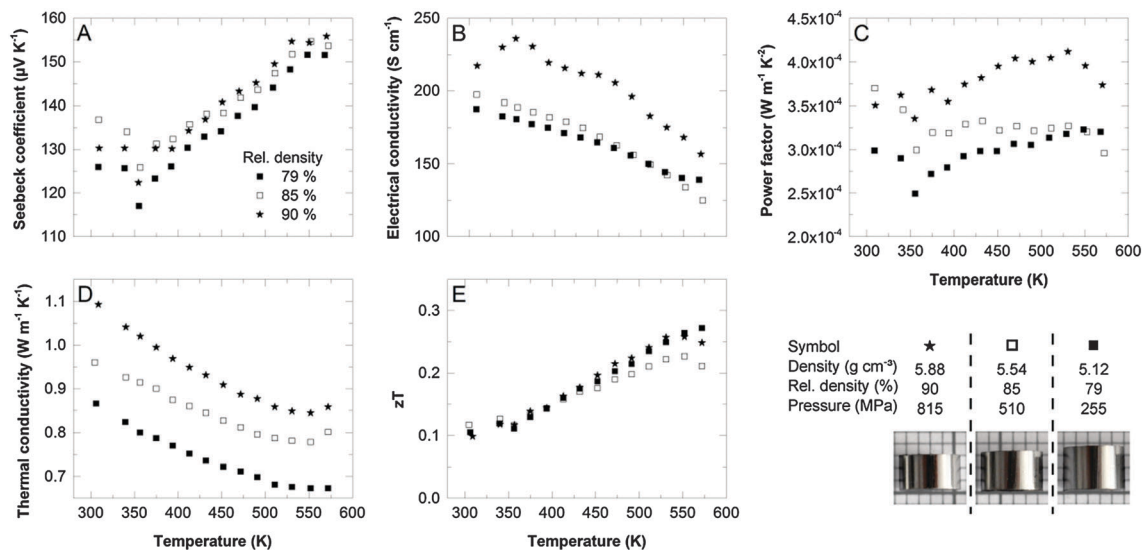This journal is © The Royal Society of Chemistry 2015

Fig. 4   Thermoelectric properties of three commercial powder samples with different relative density, fabricated by variation of compaction pressure with otherwise identical conditions as samples I and II.
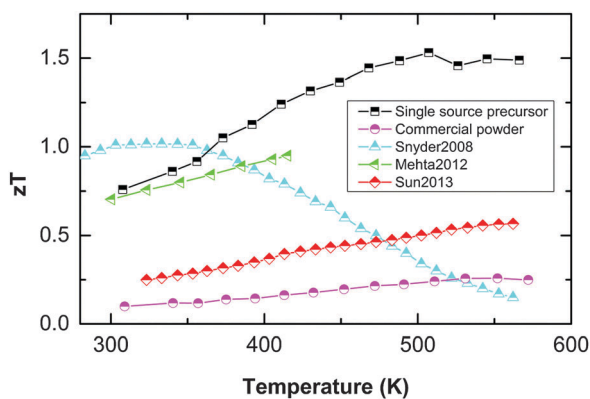

Fig. 5   Compilation of Sb_2Te_3 figure of merit data, comparing own data (single-source precursor material and commercial powder processed identically) with literature references: nanostructured Sb_2Te_3 shows best zT values around 0.6 (Sun 2013[23]). Co-doping the nanomaterial electrically with sulphur raises zT up to 1 (Mehta 2012[24]). zT values around 1 were presented in the review of Snyder and Toberer for commercial Sb_2Te_3, without further elaboration on the material's chemistry or preparation route (Snyder 2008[25]).

easily be integrated into this synthesis strategy as well as the fabrication of heterocomposite materials.[24–26]

Acknowledgements

References

1   L. E. Bell, *Science*, 2008, **321**, 1457.
2   J. P. Heremans, M. S. Dresselhaus, L. E. Bell and D. T. Morelli, *Nat. Nanotechnol.*, 2013, **8**, 471.
3   J. Yang, H.-L. Yip and A. K.-Y. Jen, *Adv. Energy Mater.*, 2013, **3**, 549.
4   N. Mingo, D. Hauser, N. P. Kobayashi, M. Plissonnier and A. Shakouri, *Nano Lett.*, 2009, **9**, 711.
5   B. Poudel, Q. Hao, Y. Ma, Y. Lan, A. Minnich, B. Yu, X. Yan, D. Wang, A. Muto, D. Vashaee, X. Chen, J. Liu, M. S. Dresselhaus, G. Chen and Z. Ren, *Science*, 2008, **320**, 634.
6   K. Biswas, J. He, I. D. Blum, C.-I. Wu, T. P. Hogan, D. N. Seidman, V. P. Dravid and M. G. Kanatzidis, *Nature*, 2012, **489**, 414.
7   C. Lorbeer, J. Cybinska and A.-V. Mudring, *J. Mater. Chem. C*, 2014, **2**, 1862.
8   J. Dupont and J. D. Scholten, *Chem. Soc. Rev.*, 2010, **39**, 1780.
9   J. Cybinska, C. Lorbeer and A.-V. Mudring, *J. Mater. Chem.*, 2012, **22**, 9505.
10 P. E. Hopkins, P. T. Rakich, R. H. Olsson, I. F. El-kady and L. M. Phinney, *Appl. Phys. Lett.*, 2009, **95**, 161902.
11 C.-J. Liu, H.-C. Lai, Y.-L. Liu and L.-R. Chen, *J. Mater. Chem.*, 2012, **22**(11), 4825.
12 J. Horák, K. Čermák and L. Koudelka, *J. Phys. Chem. Solids*, 1986, **47**, 805.
13 C. Schumacher, K. G. Reinsberg, L. Akinsinde, S. Zastrow, S. Heiderich, W. Toellner, G. Rampelberg, C. Detavernier, J. A. C. Broekaert, K. Nielsch and J. Bachmann, *Adv. Energy Mater.*, 2012, **2**, 345.
14 S. Schulz, S. Heimann, J. Friedrich, M. Engenhorst, G. Schierning and W. Assenmacher, *Chem. Mater.*, 2012, **24**, 2228.

15 G. Gupta and J. Kim, *Dalton Trans.*, 2013, **42**, 8209.

16 L. W. da Silva, M. Kaviany and C. Uher, *J. Appl. Phys.*, 2005, **97**, 114903.

17 G. A. Slack, in *CRC Handbook of Thermoelectrics*, ed. D. M. Rowe, CRC Press, Boca Raton, 1995, vol. 1, p. 407.

18 K. Richter, A. Birkner and A.-V. Mudring, *Angew. Chem., Int. Ed.*, 2010, **49**, 2431 (*Angew. Chem.*, 2010, **122**, 2481).

19 K. Richter, A. Birkner and A.-V. Mudring, *Phys. Chem. Chem. Phys.*, 2011, **13**, 7136.

20 C. Lorbeer, J. Cybinska and A.-V. Mudring, *Chem. Commun.*, 2010, **46**, 571.

21 J. Tang, H.-T. Wang, D. H. Lee, M. Fardy, Z. Huo, T. P. Russel and P. Yang, *Nano Lett.*, 2010, **10**, 4279.

22 J.-K. Yu, S. Mitrovic, D. Tham, J. Varghese and J. R. Heath, *Nat. Nanotechnol.*, 2010, **5**, 718.

23 S. Sun, J. Peng, R. Jin, S. Song, P. Zhu and Y. Xing, *J. Alloys Compd.*, 2013, **558**, 6.

24 R. J. Mehta, Y. Zhang, C. Karthik, B. Singh, R. W. Siegel, T. Borca-Tasciuc and G. Ramanath, *Nat. Mater.*, 2012, **11**, 233.

25 G. J. Snyder and E. S. Toberer, *Nat. Mater.*, 2008, **7**, 105.

26 Č. Drašar, M. Steinhart, P. Lošťák, H.-K. Shin, J. S. Dyck and C. Uher, *J. Solid State Chem.*, 2005, **178**, 1301.

10380 | *J. Mater. Chem. C*, 2015, **3**, 10375–10380

This journal is © The Royal Society of Chemistry 2015